

CHARACTERIZATION OF TISSUE-MIMICKING MATERIALS USING MAGNETIC INDUCED SHEAR WAVE

D. R. T. Sampaio, A. C. Bruno, F. W. Grillo, T. Z. Pavan and A. A. O. Carneiro

Department of physics, FFCLRP – University of Sao Paulo, Ribeirão Preto, Brazil
adilton@usp.br

Abstract:

Estimation of the tissues mechanical properties of is an important information to the pathologies diagnosis. A novel ultrasound-based methods use shear wave dispersion for this purpose. This paper describes the Magneto Motive Ultrasound (MMUs) implementation to evaluate mechanical parameters of paraffin phantoms. This technique can be applied in vivo as an alternative to biopsy. Ultrasound equipment was used with a magnetic system for generating seismic waves in paraffin phantom containing a magnetic inclusion. Consistent values of elastic and viscous modulus ($\mu_1 = 8.4 \pm 1.5$ kPa; $\mu_2 = 5.3 \pm 2.2$ Pa.s) were obtained. The evaluation of MMUs technique for estimating mechanical parameters of soft tissue was satisfactory, but for stiffer inclusions higher temporal resolution is needed.

Keywords: Ultrasound, Magneto Motive Ultrasound, Shear Wave, Paraffin Gel Phantom

Introduction

Rheology characterization of soft tissues is an important indicator of pathologies, as cancer. Ultrasound elastography is a diagnostic tool used to distinguish between pathological and healthy tissues based on the stiffness, [1]. Elastography is an alternative to biopsy, which is the gold standard [2].

Recently, ultrasound-based shear wave elasticity imaging techniques have been used to investigate soft tissues elasticity and viscosity, [3], [4]. These methods use rheological mathematical models, as Voigt model, for mechanical characterization. The Voigt model depends on shear wave frequency (ω_s), phase velocity (c_s), and viscosity attenuation (α_s) to obtain shear elasticity (μ_1) and shear viscosity (μ_2) of an viscoelastic medium with density (ρ), [5]:

$$\mu_1 = \rho c_s^2 \omega_s^2 \frac{(\omega_s^2 - \alpha_s^2 c_s^2)}{(\omega_s^2 + \alpha_s^2 c_s^2)} \quad (1)$$

$$\mu_2 = \frac{2\rho\alpha_s c_s^2 \omega_s^2}{(\omega_s^2 + \alpha_s^2 c_s^2)^2} \quad (2)$$

The magneto motive ultrasound (MMUs) uses the displacement induced by external magnetic force to locate magnetized targets inside tissue, [6]. In this case, the magnetic force produces mechanical oscillations,

inducing seismic wave propagation perpendicular to the force direction, [7].

Paraffin-gel waxes have been used as promising tissue-mimicking materials. This material has speed of sound from 1425.4 ± 0.6 to 1480.3 ± 1.7 m.s⁻¹ at room temperature (24°C) and do not suffer dehydration, [8].

In this paper we present a MMUs use as alternative to obtain mechanical parameters using shear wave dispersion in paraffin tissue-mimicking phantoms.

Materials and Methods

The in vitro studies were performed in phantom at room temperature (24°C). The phantom was a parallelepiped (80 x 80 x 25 mm) paraffin gel ($\rho_g = 850$ kg.m⁻³), [9] with a spherical (SP) ($\varnothing = 10$ mm) inclusion made of paraffin twice stiffer than the background. A second spherical ($\varnothing = 7$ mm) inclusion (SF), made of ferrite, was embedded in the phantom to be used as source to induce the seismic waves by being displaced due to the interaction with an external oscillating magnetic field. The SP is located at 35 mm of depth, and the SF at 50 mm (see Figure 1).

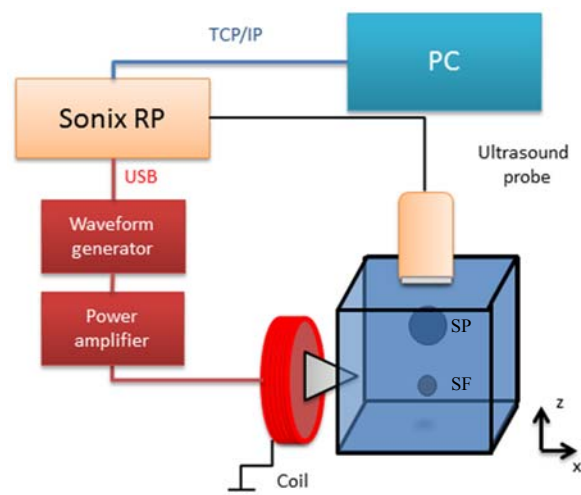


Figure 1: MMUs system used to excite a paraffin tissue mimicking phantom with a ferrite inclusion positioned under a stiffer paraffin inclusion.

A software interface, written in C++ and Qt4, was developed to load flexible sequences of acoustic acquisition synced with the magnetic excitation. The user interface runs on ultrasound equipment (Sonix RP, Ultrasonix @ 40 MHz), which also controls a function

generator (33220a, Agilent) via USB.

The scanned area ($38 \times 85 \text{ mm}^2$) was obtained using a sequential plane wave pulse-echo beamforming loaded using a 128 elements linear array transducer (L14-5/38 @ 5 MHz). The depth of 85.0 mm was divided in 32 subsectors of 4 elements operated at high frame rate (2 kHz). A single sinusoidal cycle of 100 Hz magnetic field was generated by a coil 9.1 mH ($22 \times 45 \times 89 \text{ mm}$) driven by an audio power amplifier (Dynamic 20.000, Ciclotron).

The acquired radiofrequency (RF) data was transferred to an external computer (PC), and then each subsequent RF subsector was laterally concatenated to obtain total scanned area ($38 \times 85 \text{ mm}^2$) with 2 kHz temporal resolution. The RF was processed into B-mode, also a motion estimation algorithm based on complex cross correlation (window 1.0 mm, 75% overlap) was used to get a displacement map, which contains seismic trace, which was up-sampled to 50 kHz using low pass filter interpolation ($\omega_{\text{cut}} = 200 \text{ Hz}$), and then was applied Hilbert transform to obtain phase information.

For a fixed time position, the phase change $\frac{\Delta\phi}{\Delta z}$ was obtained using linear regression to estimate phase velocity, Eq. (3).

$$c_s = \omega_s \frac{\Delta z}{\Delta\phi} \quad (3)$$

The total attenuation of shear wave is the sum of geometric losses (α) and material viscosity (α_s), [5], [10]. The amplitude decay along path $A(z)$ was used to estimate total attenuation applying exponential regression, Eq. (4).

$$\alpha_{\text{total}} = \frac{\ln\left[\frac{A(z_1)}{A(z_2)}\right]}{\Delta z} \quad (4)$$

The quality of the regressions was evaluated using R-squared, and only values up to 90% were used in the calculation of the shear wave attenuation and velocity.

Results

The phantom temperature was $23.5 \pm 1.5 \text{ }^\circ\text{C}$ measured with infrared thermometer model (TR-300, Equitherm), with emissivity set to 0.95. Figure 2 shows a comparison between B mode and displacement map during propagation of shear wave generated by SF oscillation, 35 ms after magnetic excitation. The seismic waves were evaluated using the ROI (red box) shown in Figure 2 (a) and (b).

The shear wave propagation in the ROI is showed in Figure 3. The shear wave amplitude decay was fitted using Eq.(4) to estimate the attenuation (Figure 4).

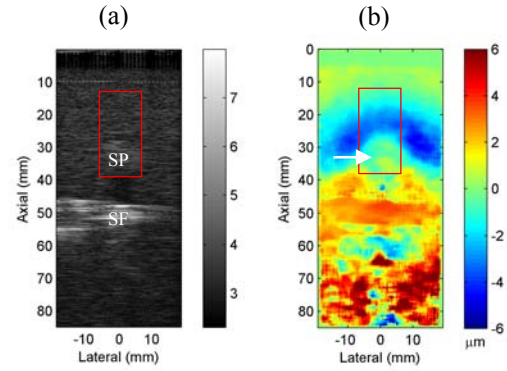


Figure 2: (a) B mode and (b) 2D displacement map during the propagation of the shear wave. In the displacement map the SP bounds can be observed. (arrow), the ROI used to estimate velocity and attenuation are displayed in both images.

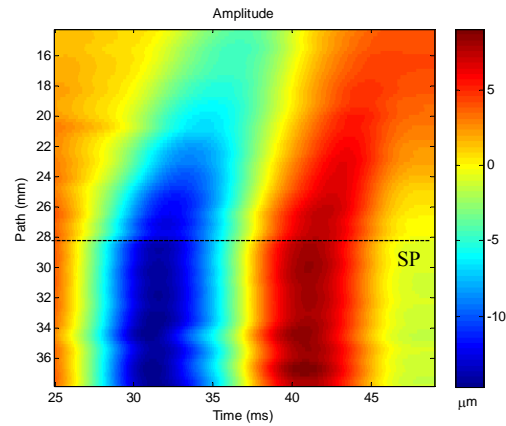


Figure 3: Shear wave propagation in the ROI. The amplitude change along path inside SP (dashed) is lower than outside indicating different attenuation and velocities.

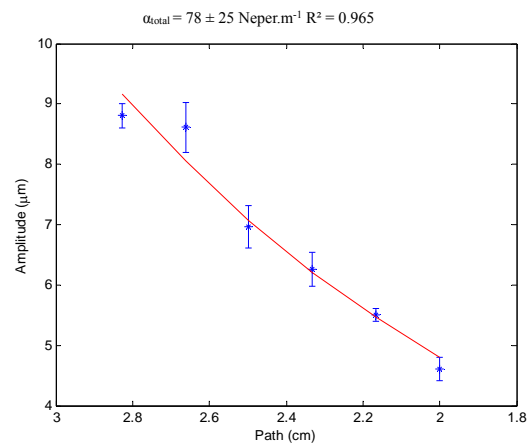


Figure 4: Shear wave total attenuation curve in a region outside SP.

The phase change during seismic wave propagation obtained using Hilbert transform is showed in Figure 5, also velocity at 35 ms (solid line) was estimated using

Eq. (3), Figure 6.

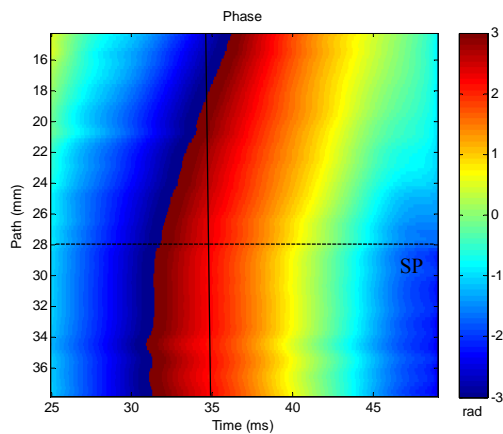


Figure 5: Phase of shear wave in the ROI obtained using Hilbert approach. The regions separated by a horizontal dashed line were evaluated using linear regressions at 35 ms.

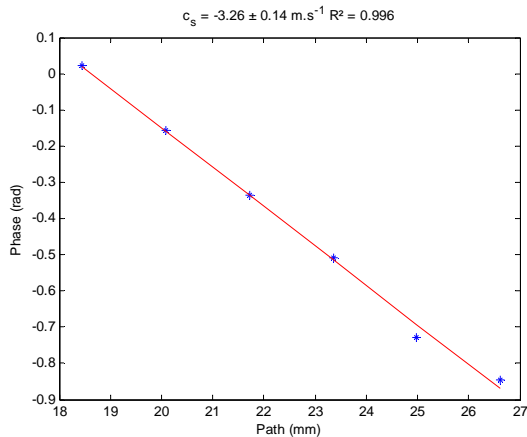


Figure 6: Linear regression used to obtain shear wave velocity at 35 ms, along 7.5 mm.

The total attenuation (TA) of shear wave obtained is $\alpha_{total} = 78 \pm 25$ Neper.m⁻¹. The geometric attenuation (GA) was estimated simulating, [10], a pure elastic medium ($\rho_g = 850$ kg.m⁻³), where a shear wave propagates with the velocity of $c_s = 3.26 \pm 0.14$ m.s⁻¹ (Figure 6) obtaining $\mu_1 = 9.0 \pm 0.3$ kPa and $\alpha = 32$ Neper.m⁻¹, and then a ratio of TA:GA is used to estimate $\alpha_s = 2.5 \pm 0.8$ Neper.m⁻¹. From Eq.(1-2) we obtained elastic and viscosity modulus (Table 1).

Table 1: Shear wave velocity, attenuation, elastic modulus and viscosity modulus for paraffin.

ω (Hz)	c_s (ms ⁻¹)	α_s (Neper.m ⁻¹)	μ_1 (kPa)	μ_2 (Pa.s)
100	3.26 ± 0.14	2.5 ± 0.8	8.4 ± 1.5	5.3 ± 2.2

Discussion

The experiments were conducted using 100 Hz of excitation which provided a shear wave with significant SNR to evaluate region outside SP, (Figure 2). The mechanical parameters obtained for paraffin gel using visco-elastic equations (1) and (2) are consistent, [4], [10]–[12], however, this methodology can't evaluate the SP region. One explanation for this inability is the temporal resolution of 2 kHz, which was, possibly, insufficient to evaluate the stiffer inclusions. Difficulties of sequential beamforming could be overcome with parallel beamforming ultrasound systems, [13].

Conclusion

We have presented the MMUs system for mechanical characterization using shear wave dispersion. Experiments with variations of stiffness using different excitation frequencies should be performed to obtain velocities range of technique. A possible application in vivo is the use of MMUs system with Brachytherapy seeds for shear wave dispersion to differentiate ill tissues during treatment.

Acknowledgments

We acknowledge CAPES, CNPq and FAPESP for financial support, Figlabs company for encouraging application of scientific development in society and to Mr. Carlos Renato da Silva for technical support.

References

- [1] J. Ophir, S. K. Alam, B. Garra, F. Kallel, E. Konofagou, T. Krouskop, e T. Varghese, "Elastography: ultrasonic estimation and imaging of the elastic properties of tissues", in *In Proc. Instn. Mech. Engrs., Part H: Journal of Engineering in Medicine*, 1999, p. 203–233.
- [2] L. Pallwein, M. Mitterberger, P. Struve, W. Horninger, F. Aigner, G. Bartsch, J. Gradl, M. Schurich, F. Pedross, e F. Frauscher, "Comparison of sonoelastography guided biopsy with systematic biopsy: impact on prostate cancer detection", *Eur. Radiol.*, vol. 17, n° 9, p. 2278–2285, set. 2007.
- [3] P. Song, H. Zhao, A. Manduca, M. W. Urban, J. F. Greenleaf, e S. Chen, "Comb-Push Ultrasound Shear Elastography (CUSE): A Novel Method for Two-Dimensional Shear Elasticity Imaging of Soft Tissues", *IEEE Trans. Med. Imaging*, vol. 31, n° 9, p. 1821–1832, set. 2012.
- [4] C. Amador, M. W. Urban, S. Chen, Q. Chen, K.-N. An, e J. F. Greenleaf, "Shear elastic modulus estimation from indentation and SDUV on gelatin phantoms", *IEEE Trans. Biomed. Eng.*, vol. 58, n° 6, p. 1706–1714, jun. 2011.
- [5] H. Zhao, M. Urban, J. Greenleaf, e S. Chen, "Elasticity and viscosity estimation from shear wave velocity and attenuation: A simulation study",

- in *2010 IEEE Ultrasonics Symposium (IUS)*, 2010, p. 1604–1607.
- [6] A. Colello Bruno, T. Z. Pavan, O. Baffa, e A. A. Oliveira Carneiro, “A hybrid transducer to magnetically and ultrasonically evaluate magnetic fluids”, *IEEE Trans. Ultrason. Ferroelectr. Freq. Control*, vol. 60, nº 9, p. 2004–2012, 2013.
- [7] T. Z. Pavan, D. R. T. Sampaio, A. A. O. Carneiro, e D. T. Covas, “Ultrasound-based transient elastography using a magnetic excitation”, in *Ultrasonics Symposium (IUS), 2012 IEEE International*, 2012, p. 1846–1849.
- [8] S. L. Vieira, T. Z. Pavan, J. E. Junior, e A. A. O. Carneiro, “Paraffin-Gel Tissue-Mimicking Material for Ultrasound-Guided Needle Biopsy Phantom”, *Ultrasound Med. Biol.*, vol. 39, nº 12, p. 2477–2484, dez. 2013.
- [9] G. W. C. Kaye e T. H. Laby, *Tables of physical and chemical constants*. Longman, 1995.
- [10] S. Catheline, F. Wu, e M. Fink, “A solution to diffraction biases in sonoelasticity: The acoustic impulse technique”, *J. Acoust. Soc. Am.*, vol. 105, nº 5, p. 2941–2950, maio 1999.
- [11] K. Nightingale, “Acoustic Radiation Force Impulse (ARFI) Imaging: a Review”, *Curr. Med. Imaging Rev.*, vol. 7, nº 4, p. 328–339, nov. 2011.
- [12] M. M. Nguyen, S. Zhou, J. Robert, V. Shamdasani, e H. Xie, “Development of Oil-in-Gelatin Phantoms for Viscoelasticity Measurement in Ultrasound Shear Wave Elastography”, *Ultrasound Med. Biol.*, vol. 40, nº 1, p. 168–176, jan. 2014.
- [13] P. J. Kaczkowski e R. E. Daigle, “The Verasonics ultrasound system as a pedagogic tool in teaching wave propagation, scattering, beamforming, and signal processing concepts in physics and engineering.”, *J. Acoust. Soc. Am.*, vol. 129, nº 4, p. 2648–2648, abr. 2011.